

J Geod (2013) 87:427–437
DOI 10.1007/s00190-013-0616-5

ORIGINAL PAPER

Stochastic modeling of high-stability ground clocks in GPS analysis

Kan Wang · Markus Rothacher

Received: 21 June 2012 / Accepted: 22 January 2013 / Published online: 19 March 2013
© Springer-Verlag Berlin Heidelberg 2013

Abstract In current global positioning system (GPS) applications, receiver clocks are typically estimated epoch-wise in the data analyses even for clocks with high performance like Hydrogen-masers (H-maser). Applying an appropriate clock model for high-stability receiver clocks should, in view of the strong correlation between the station height and the clock parameters, significantly improve the positioning results. Recent experiments have shown that modeling the deterministic behavior of high-quality receiver clocks can improve the kinematic precise point positioning considerably. In this paper, well-behaving ground clocks are studied in detail applying constraints between subsequent and near-subsequent clock parameters. The influence of different weights for these relative clock constraints on the positioning quality, especially on the height, is investigated. For excellent clocks, an improvement of up to a factor of 3 can be obtained for the repeatability of the kinematic height estimates. This may be essential to detect small but sudden changes in the vertical component (e.g., caused by earthquakes). Troposphere zenith path delays (ZPD) are also heavily correlated with the receiver clock estimates and station heights. All these parameters are usually estimated simultaneously. We show that the use of relative clock constraints allows for a higher time resolution of the ZPD estimates (smaller than 2 h) without compromising the quality of the kinematic height estimates.

Keywords Stochastic clock model · GPS kinematic PPP · High-performance atomic clock · Troposphere

K. Wang (✉) · M. Rothacher
Institute of Geodesy and Photogrammetry, ETH Zurich,
Schafmattstr. 34, 8093 Zurich, Switzerland
e-mail: wangk@ethz.ch

M. Rothacher
e-mail: markus.rothacher@ethz.ch

1 Introduction

In the present-day analyses of global navigation satellite system (GNSS) data, the receiver clocks and satellite clocks are typically estimated as independent parameters for each measurement epoch in the least-squares adjustment. The resulting large number of clock parameters are strongly correlated with troposphere Zenith Path Delays (ZPD) parameters and the station height (Dach et al. 2003; Rothacher and Beutler 1998). It can be expected that, if the quality of the high-performance receiver clocks could be fully exploited with an appropriate deterministic and stochastic model, the solutions of other parameters, especially the kinematic station height estimates, should become more stable and more accurate because of the strong correlation between the clock parameters and the station height.

The idea of a detailed stochastic modeling of receiver and satellite clocks is not really new. During the 1980s, colleagues at Jet Propulsion Laboratory (JPL) modeled clock and troposphere parameters using different stochastic processes in order to improve GNSS-relevant parameters like orbits (Lichten and Border 1987). At that time, however, the impact of a sophisticated clock model was marginal due to the fact that the large majority of the ground-based and space-borne clocks was not sufficiently accurate and stable compared to the phase measurement noise of 1–2 mm (3.3–6.7 ps) to allow for such approaches.

In the last 20 years, more and more stable atomic clocks are connected to GNSS receivers in the International GNSS Service (IGS) (Dow et al. 2009) network and used for time and frequency transfer accompanied with the stronger connections between different timing labs and the IGS stations (Ray and Senior 2003). Such a development also takes place in space, where satellites are equipped with better and better clocks. Examples are the Hydrogen-maser

(H-maser) on GIOVE-B (Galileo In-Orbit Validation Element), see [Montenbruck et al. \(2012\)](#), and the modified rubidium clock on GPS-IIF SVN62 ([Dupuis et al. 2010](#)). In recent years, investigations concerning clock modeling came to into focus again. [Weinbach and Schön \(2011\)](#) have shown that an improvement in the vertical component of kinematic Precise Point Positioning (PPP) ([Zumberge et al. 1997](#)) by up to 70 % can be expected by applying a simple deterministic clock model. They demonstrated that loose relative constraints on clock parameters may improve the vertical component in the case of pseudo-range kinematic solutions as well ([Weinbach and Schön 2009](#)).

Because of the high quality of the H-masers available nowadays, the constraints between subsequent and near-subsequent clock epochs (the so-called relative constraints) can also be applied for phase positioning. An appropriate weighting of these relative constraints depending on the individual clock performance is very important to obtain optimal kinematic positions. Constraining the clocks too strongly (e.g. neglecting environmental influences and hardware delay variations) may lead to a degradation of the kinematic positioning results. In this study here, detailed investigations concerning the weight of the relative constraints on subsequent and near-subsequent (between every three epochs) clock parameters are performed and the benefit in kinematic positioning results using phase (and heavily down weighted code) observations is assessed.

In addition, the global positioning system (GPS) data were analyzed to study whether the temporal resolution of troposphere parameters can be increased when constraining clocks to further improve the kinematic height estimates.

2 Deterministic and stochastic modeling of the receiver clock

In our approach we assume that the receiver clock can be described by a simple deterministic model (e.g., low-order polynomial) and a stochastic model:

$$\begin{aligned} \text{clk}(t_i) &= a_m \cdot (t_i - t_0)^m + \dots + a_1 \cdot (t_i - t_0) + a_0 + p(t_i), \\ \text{clk}(t_{i+1}) &= a_m \cdot (t_{i+1} - t_0)^m + \dots + a_1 \cdot (t_{i+1} - t_0) \\ &\quad + a_0 + p(t_{i+1}), \end{aligned} \tag{1}$$

where $\text{clk}(t_i)$ represents the receiver clock correction for measurement epoch i , a_m, \dots, a_1, a_0 are the coefficients of the low-degree polynomial, and $p(t_i)$ is the stochastic clock parameter for measurement epoch i .

The deviations of a clock can be divided into two categories, namely, the systematic effects such as the time offset, the frequency offset and the frequency drift, as well as the non-deterministic random errors such as white noise, flicker noise and random-walk noise ([Allan 1987](#)). A study concerning the deterministic models of high-precision clocks and of

their impact on other GPS-related parameters was done parallel to this study. The results have shown that the simplest deterministic model, namely, a linear polynomial, works the best for stabilizing the kinematic height estimates ([Orliac et al. 2012](#)). In this study, therefore, a linear polynomial is used. The clock parameters to be estimated from the GPS data are the coefficients a_1, a_0 and the stochastic clock parameters $p(t_i)$. The stochastic clock parameters $p(t_i)$ represent the deviations of the real clock from the linear polynomial given by the coefficients a_1 and a_0 in Eq. 1. The size of these deviations $p(t_i)$ depends on the clock quality. The stochastic clock parameters of subsequent epochs t_i and t_{i+1} can be constrained using a pseudo-observation with the weight $P_{i,i+1}$:

$$p(t_i) - p(t_{i+1}) = 0, \quad P_{i,i+1} = \frac{\sigma_0^2}{\sigma_{\text{rel}}^2}, \tag{2}$$

where σ_0 and σ_{rel} represent the a priori standard deviation of unit weight, i.e., the standard deviation of the GPS phase observations, and the standard deviation of the relative constraint between the two subsequent epochs, respectively. The weight of the relative constraints is the most important quantity in the stochastic model. In order to be consistent with the unit of σ_0 , σ_{rel} is expressed in millimeter in this paper.

Similar constraints can also be added for near-subsequent epochs. In general, the stochastic behavior between the i th and the $(i + n)$ th epoch is then constrained according to:

$$p(t_i) - p(t_{i+n}) = 0, \quad P_{i,i+n} = \frac{\sigma_0^2}{\sigma_{\text{rel},n}^2}, \tag{3}$$

where $\sigma_{\text{rel},n}$ stands for the standard deviation of the relative constraint between near-subsequent epochs t_i and t_{i+n} . The weight $P_{i,i+n}$ can thereby be derived from, e.g., the Modified Allan Deviation (MDEV) of the clock records from the Center for Orbit Determination in Europe (CODE). The MDEV is, like the traditional Allan deviation (ADEV), a measure of the frequency stability and is able to distinguish between the white phase noise and the flicker phase noise ([Allan and Barnes 1981](#)). $\sigma_{\text{rel},n}$ here is the product of the MDEV value at the corresponding averaging time ($\sigma_{\text{MDEV},n}$), the speed of light (c) and the averaging time (τ_n) itself:

$$\sigma_{\text{rel},n} = \sigma_{\text{MDEV},n} \cdot c \cdot \tau_n. \tag{4}$$

Since the drift a_1 and the offset a_0 of the linear polynomial are estimated as non-epoch parameters simultaneously with the stochastic quantities $p(t_i)$, weak absolute constraints with a small weight P_i have to be put on the stochastic parameters $p(t_i)$ to avoid the singularities between the offset,

the drift and the stochastic parameters. These absolute constraints have the form

$$p(t_i) = 0, \quad P_i = \frac{\sigma_0^2}{\sigma_{\text{abs}}^2}, \quad (5)$$

where σ_{abs} represents the RMS of the absolute constraints.

For network solutions involving a huge number of parameters, the epoch-parameters are usually pre-eliminated for increasing the computation efficiency (Jäggi et al. 2011). Ge et al. (2006) has introduced a procedure to pre-eliminate the ambiguity parameters for both real-valued and ambiguity-fixed solutions and accelerated the computation for huge network solutions significantly. To limit the required computer resources, clock parameters are efficiently eliminated at every epoch. If relative constraints are applied, a rather complex pre-elimination and back-substitution scheme has to be used (and was implemented) for the least-squares adjustment that also works for near-subsequent epoch parameters. The stochastic clock parameters are efficiently pre-eliminated at every epoch in order to limit the computation time. Before pre-eliminating a specific epoch, the stochastic clock parameters of the subsequent and near-subsequent epochs to be constrained have to be considered. After determination of all the non-epoch parameters, a back-substitution is performed starting backwards from the last epoch. All the relevant information required for this back-substitution has to be stored step-by-step during the pre-elimination process. In this way, relative clock constraints can also be applied for relatively big regional network or even global solutions.

3 Identification of good H-masers

At present there are over 130 IGS stations equipped with high-performance atomic clocks. Figure 1 shows the global distribution of these clocks on April 1st, 2012 including 68 H-masers, 43 cesium and 26 rubidium clocks (CLKLOG 2012).

We can expect that the application of relative constraints on clock parameters is most beneficial for stations with very stable H-masers compared to cesium and rubidium clocks (Allan 1987). The clock values of H-masers with jumps, equipment changes or other problems can only be estimated epoch-wise as it has been done so far. A rough characterization of these H-masers can be obtained from the analysis of the clock estimates, which are freely available in the IGS, the CODE or the European Space Agency (ESA) stored in clock RINEX files (Ray and Gurtner 2010). In order to make sure that the clock estimates used for the clock characterization represent the actual clock behavior as precisely as possible, all clock estimates were referenced to the IGS time scale (IGST) (Wang and Rothacher 2011; Senior et al. 2003). One way to characterize the H-masers is the empirical RMS of epoch-to-epoch differences σ_{emprrel} (the so-called empirical

relative sigma), that can be calculated based on the clock records in these clock RINEX files according to

$$\sigma_{\text{emprrel}} = \sqrt{\frac{\sum_{i=1}^{n-1} (\text{clk}(t_{i+1}) - \text{clk}(t_i))^2}{n-1}}, \quad (6)$$

where n represents the number of processed epochs. It should be noticed that the detected clock jumps or problems here are mainly concerning the GPS receiver, the installation and clock adjustments rather than the H-Maser itself. For such bad behaviors, the clock values usually exceed the GPS measurement noise and allow thus the identification and exclusion of the misbehaving H-Masers.

As an example, Fig. 2 shows the daily empirical relative sigma σ_{emprrel} of the H-maser located at station CEDU (CEDUNA, Ceduna, Australia) in February 2011 and, for February 15, 2011, the clock residuals after removing a linear polynomial. The values of σ_{emprrel} amount to around 60–70 ps for most of the days in February 2011, but may sometimes reach more than 150 ps. The big clock jumps on February 15, 2011 is, e.g., the cause of the relatively big empirical relative sigma of about 200 ps.

The values σ_{emprrel} are a good measure of the clock quality, especially for detecting clock jumps. In our analyses of a specific H-maser clock, the days with an empirical relative sigma σ_{emprrel} bigger than 100 ps were excluded. Figure 3 shows the mean values of σ_{emprrel} for some well-behaving H-masers in February 2011, excluding the days with data gaps and the days with bad σ_{emprrel} values. It can be seen that most H-masers are performing very well with a mean σ_{emprrel} smaller than 30 ps (9 mm).

4 Estimation of kinematic station coordinates with real data

In order to assess the effect of relative clock constraints, experiments with PPP were performed using a modified version of the Bernese GPS Software (Dach et al. 2007). The kinematic (i.e. epochwise) coordinates of a static station equipped with a well-behaving H-maser were estimated together with the receiver clock parameters with a sampling rate of 300 s over a time span of 24 h. The wet part of the troposphere ZPD was estimated as a piece-wise linear function with a 2 h resolution and the wet Vienna Mapping functions 1 (VMF1) (Boehm et al. 2006). In addition, troposphere gradients were estimated with a resolution of 24 h. The satellite clocks were fixed to high-rate precise clocks from CODE (Bock et al. 2009; Dach et al. 2009; Hugentobler 2004). Since the investigated stations are static, the standard deviations of the estimated kinematic coordinates are considered as a measure for the appropriateness of different clock constraints. Clocks with adjustments or huge jumps were excluded based on the empirical relative sigmas σ_{emprrel}

Fig. 1 Global distribution of IGS stations with high-performance atomic clocks

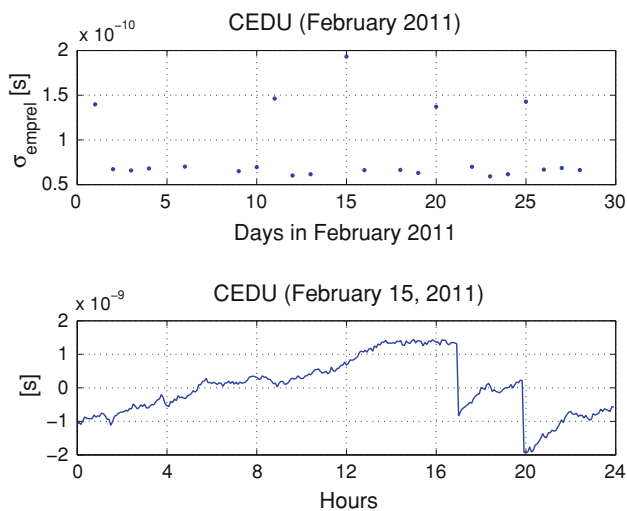
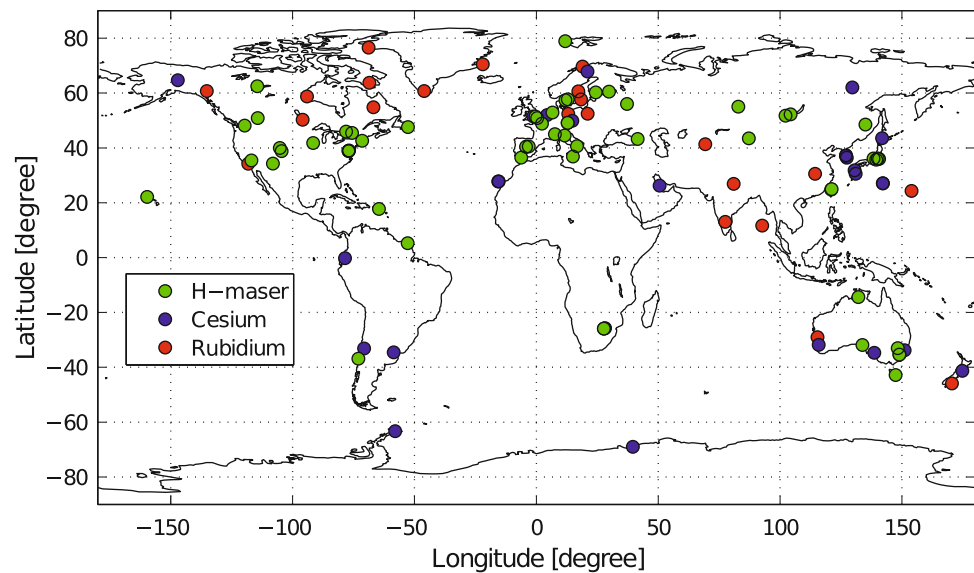


Fig. 2 Empirical relative sigma σ_{emptrel} for the H-maser clock at station CEDU in February 2011 (*top*) and the residuals for this clock after removing a linear polynomial on February 15, 2011 (*bottom*). The CODE clock RINEX files were used for the plots

(see Eq. 6) derived from the epoch-to-epoch differences of the GPS clock estimates.

Figure 4 shows the effect of relative constraints of different strengths on the H-maser clock estimates at station ONSA (ONSALA, Onsala, Sweden) on February 1st, 2011. The clock estimates without any constraints are shown in blue, while the red, green and magenta lines represent the clock estimates with increasing relative constraints. Finally, applying very strong constraints results in an almost straight line (black). We thus see that, as expected, increasing the relative constraints forces the clock estimates to converge towards a straight line.

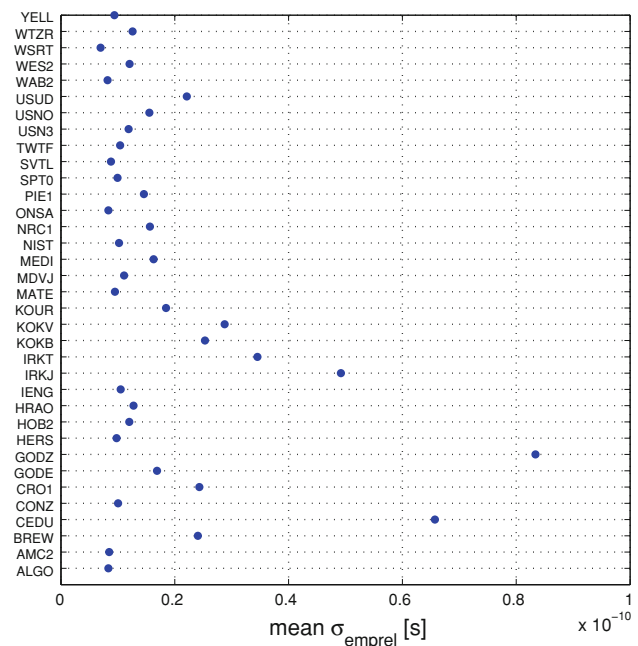


Fig. 3 Mean empirical relative sigma σ_{emptrel} for some H-masers in February 2011. The IGS/CODE/ESA clock RINEX files were used for the plot

Figure 5 shows the corresponding kinematic height estimates for station ONSA on February 1st, 2011. As in Fig. 4, the blue line indicates the kinematic solution without any clock constraints, while the red, green and magenta lines represent the kinematic height estimates with increasing relative constraints. It can be observed that the kinematic height estimates of the static station ONSA are significantly improved by applying relative clock constraints, e.g., up to a factor of 2. This improvement of the height repeatability (see standard deviations σ_H in the legend of Fig. 5) is

Fig. 4 Clock estimates for station ONSA using different relative constraints between subsequent clock epochs on February 1st, 2011

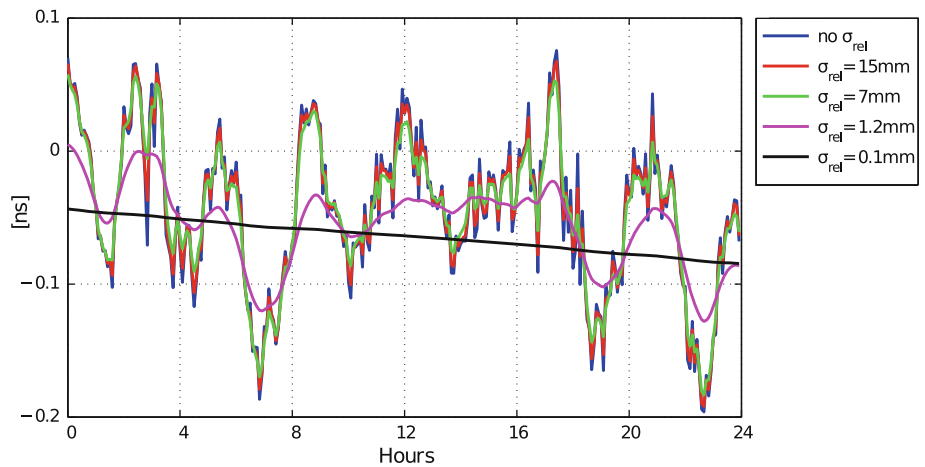
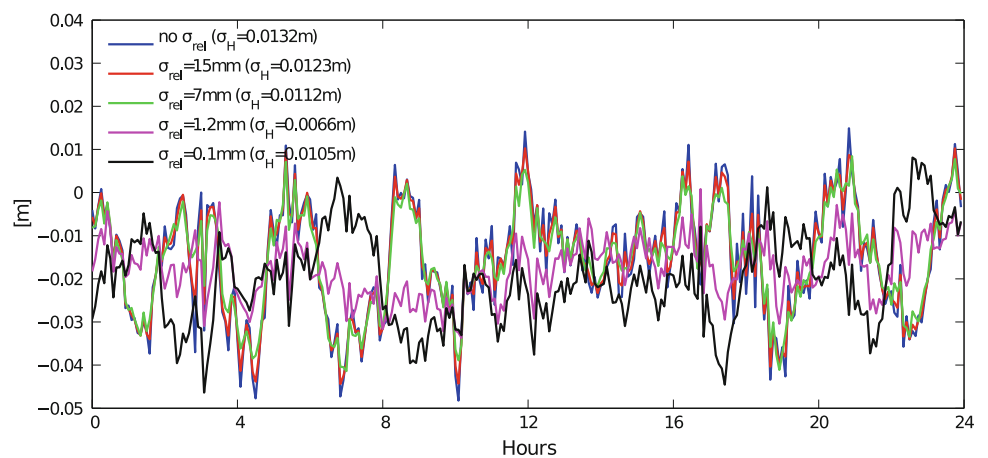


Fig. 5 Kinematic height estimates for station ONSA on February 1st, 2011 using different relative constraints between subsequent clock epochs



a consequence of relative constraints together with the high correlations between the clock parameters and the height estimates. This is especially important, since the height estimates from GPS are typically much less precise than the horizontal components. The black line using very strong relative constraints shows, however, a degradation of the positioning results in the vertical direction.

To study the impact of the relative constraints in more detail, a large series of kinematic solutions were produced decreasing σ_{rel} in steps of 0.1 mm from 20 mm down to 0.1 mm. Figure 6 shows these results, i.e., the direct relationship between the weights of the relative constraints between subsequent clock parameters and the standard deviation of the kinematic coordinates for station ONSA on February 1st, 2011, in all three directions (North, East, Up). Starting with very weak constraints, the standard deviation of the kinematic height estimates (red line) decreases with increasing relative constraint (i.e., decreasing relative sigma), and shows a minimum at a relative constraint of about 1.2 mm (4 ps). With stronger relative constraints the estimated clock values cannot represent the clock variations anymore and the results are degraded. As opposed to the height estimates,

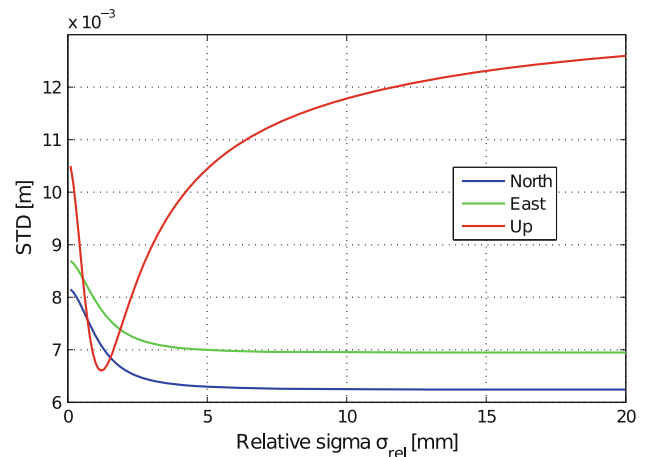


Fig. 6 Standard deviation of the kinematic coordinates for station ONSA with different relative constraints on February 1st, 2011

the horizontal coordinates are not improved by constraining the clock parameters. A significant degradation can be observed especially for a relative sigma smaller than 2 mm (6.7 ps). The relative sigma σ_{rel} of about 1.2 mm (4 ps), which leads to the best kinematic height estimates, degrades

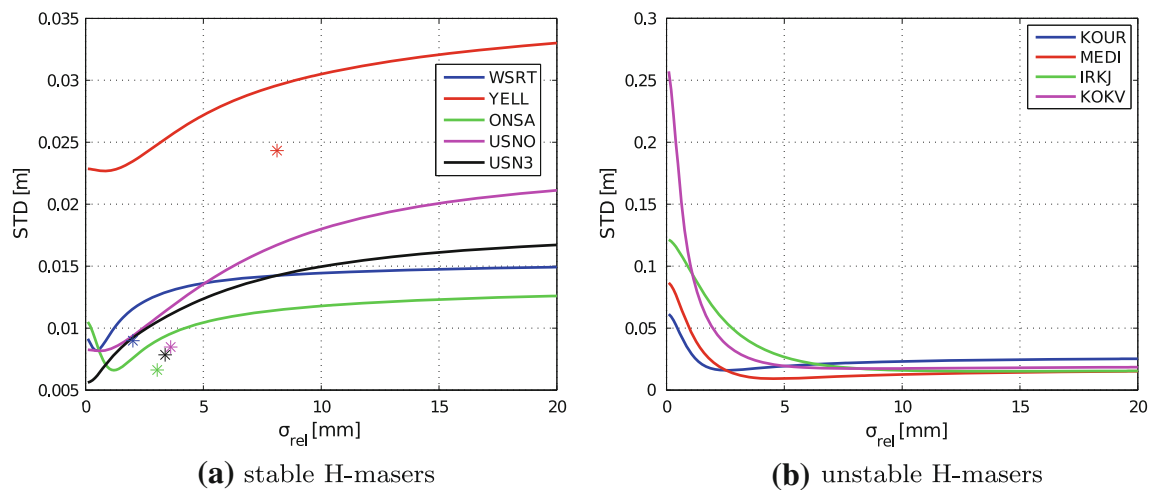


Fig. 7 Stability improvements of kinematic height estimates for some **a** stable and **b** unstable H-masers on February 1st, 2011, using different relative constraints

at the same time the horizontal coordinates and is, thus, not the optimal choice. The reason for the degradation of the kinematic horizontal coordinates with relative sigmas bigger than 1.2 mm is not clear.

Figure 7a shows the improvements in the kinematic height estimates for some well-behaving H-masers on February 1st, 2011. The solid lines represent the standard deviations of the kinematic height estimates using different relative constraints between subsequent epochs. These epoch-to-epoch relative constraints can improve the stability of kinematic height estimates reaching an optimum for a very small relative sigma σ_{rel} between 0 and 2 mm (0 and 6.7 ps). The improvement reaches a factor of about 2 to 3. However, this conclusion only holds for very stable H-masers (e.g. clock with σ_{empr} smaller than 15 ps). For H-masers that are not that stable, the standard deviations of the kinematic height estimates grow rapidly after reaching a relative sigma σ_{rel} smaller than 2 mm (see Fig. 7b). Only very weak relative constraints may be considered for such clocks (for KOKV 8.5 mm and for IRKJ 14.2 mm).

The asterisks in Fig. 7a represent the standard deviations using not only relative constraints between subsequent epochs (called $\sigma_{rel,1}$), but also between near-subsequent epochs (every third subsequent epoch, called $\sigma_{rel,2}$). The relative sigma values $\sigma_{rel,1}$ and $\sigma_{rel,2}$ have been derived from the MDEV of the CODE clock records, and the x-coordinate of the asterisks in Fig. 7a is set to be the relative sigma $\sigma_{rel,1}$, i.e. the product of the MDEV value at 300 s derived from the clock records, the speed of light and the averaging time of 300 s. The three-epoch constraints cannot be directly compared with the optimal standard deviation of the epoch-to-epoch constraints because the CODE clock records used for MDEV comprise the measurement noise, but they also improve the stability of the kinematic height estimates significantly.

Table 1 summarizes the improvements obtained in the kinematic height estimates for some H-maser clocks on February 1st, 2011. The clocks are sorted by their quality. The quality is based on the standard deviations σ_{STD} computed after removing a linear polynomial from the corresponding clock records (column 2). The empirical relative sigma σ_{empr} is listed in the third column. The data from different institutes (IGS/CODE/ESA) were used to give a complete list of the evaluation for the given clocks. The corresponding agency is indicated with the first letter (see column 2). The fourth column and the fifth column document the standard deviation of the kinematic height estimates without constraints (STD_0) and with the optimal constraints (STD_{min}), which generates the most stable kinematic height estimates. The sixth column contains the standard deviation of the kinematic height estimates using relative constraints between three consecutive epochs. The seventh column lists the values σ_{rel} , which lead to the minimal standard deviation of the kinematic height estimates for the corresponding station (see Fig. 7). It should be noted that the range of σ_{rel} values tested started with a value of 0.1 mm. Even stronger relative constraints have not been studied. The improvement factor f of the kinematic height estimates (column 8) has been calculated based on

$$f = \frac{STD_0}{STD_{min}}. \quad (7)$$

From Table 1 we see that for very stable H-masers the kinematic height estimates could be improved by up to a factor of 2 to 3 by applying relative constraints between 0 and 2 mm (0 and 6.7 ps). If the best relative sigma to be used is not known, an epoch-to-epoch relative constraint of 2 mm or a near-subsequent constraint derived from a MDEV plot may be a safe way to stabilize the kinematic solutions in the vertical direction. The improvement that can be reached

Table 1 Improvements of kinematic height estimates for some H-masers using relative constraints between subsequent and near-subsequent clock parameters on February 1, 2011

Station	Clock estimates		Kinematic height estimates				f
	σ_{STD} (ps)	σ_{emprcl} (ps)	STD_0 (m)	STD_{min} (m)	STD_{Covar} (m)	σ_{rel} (mm)	
WSRT	12.9 (I)	6.2	0.0153	0.0082	0.0090	0.5	1.87
ONSA	22.1 (I)	10.9	0.0132	0.0066	0.0066	1.2	2.00
USNO	22.9 (I)	10.6	0.0232	0.0082	0.0085	0.6	2.84
USN3	23.3 (I)	10.0	0.0196	0.0056	0.0078	0.1	3.50
YELL	23.5 (C)	22.0	0.0687	0.0227	0.0243	0.8	3.03
CRO1	32.8 (I)	23.2	0.0356	0.0158	–	0.1	2.25
AMC2	33.7 (I)	7.9	0.0192	0.0159	0.0165	2.2	1.21
HRAO	39.1 (I)	12.0	0.0225	0.0114	–	0.6	1.98
HOB2	40.5 (I)	15.5	0.0240	0.0098	0.0139	1.2	2.44
TWTF	44.6 (I)	9.8	0.0179	0.0108	0.0109	1.2	1.66
ALGO	45.3 (I)	6.5	0.0108	0.0057	0.0058	1.0	1.89
BREW	55.3 (I)	23.5	0.0153	0.0094	–	1.8	1.63
KOUR	241.1 (I)	20.0	0.0266	0.0159	0.0159	2.5	1.67
MEDI	342.2 (I)	18.0	0.0177	0.0092	–	4.6	1.90
IRKJ	416.2 (I)	55.1	0.0178	0.0152	–	14.2	1.17
KOKV	982.7 (E)	33.9	0.0198	0.0173	–	8.5	1.14

The IGS/CODE/ESA clock RINEX files were used for generating the σ_{STD} and σ_{emprcl}

depends heavily on the clock quality. Clocks with an unstable or unknown behavior are not suitable for clock modeling. Constraining such clocks may lead to much worse results. It should be mentioned that very strong and unrealistic weights for relative constraints ($\sigma_{rel} \ll 2\text{ mm}$) may also make things worse even for very stable H-masers (see Fig. 7). The reason for this may be related to the noise level of the observations and the simultaneous estimation of other parameters (e.g., troposphere parameters). Apart from that, real clock variations may not be adequately modeled with too strong clock constraints. Looking carefully at Table 1 we can see that the improvement factor f that can be achieved in the repeatability of the kinematic height estimates is not a simple function of the clock quality given by the deviations from a straight line (σ_{STD}) or the size of the epoch-to-epoch clock differences as defined by σ_{emprcl} . Besides σ_{STD} and σ_{emprcl} other factors like multipath, antenna environment seem to play a major role, too. A bad observation geometry or a limited number of the phase observations may strongly degrade the kinematic estimates in the case no clock constraint is applied (e.g. YELL in Table 1). The relative sigma between subsequent and near-subsequent epochs $\sigma_{rel,n}$ (see Eq. 4) derived from the CODE clock records and the optimal relative clock constraints that we obtained here (see Table 1) do not necessarily correspond to the real clock behavior. They are also influenced by the measurement noise, the antenna environment, multipath and troposphere variations.

Let us have a look now at the optimal values for the relative constraints over a longer time period. Fig. 8a shows

these optimal values for five very stable H-masers for all days in February 2011. The variations for an individual clock strongly depend on the clock behavior on the corresponding day. For most of the days in February 2011 the best σ_{rel} values are smaller than 2 mm (6.7 ps), while some outliers can also be observed. Taking the H-maser clock at station YELL (YELL CACS-GSD, Yellowknife, Canada), for example, two outliers on February 6, 2011 and February 25, 2011 can be observed in Fig. 8a, indicating an unstable clock behavior. For comparison, Fig. 8b shows σ_{emprcl} (see Eq. 6) based on the CODE clock RINEX files for the H-maser at station YELL in February 2011. We see that the days with a high value of σ_{emprcl} correspond to the outliers in Fig. 8a. Very strong constraints on clock parameters on these 2 days would lead to a degradation of the positioning results.

Figure 9 shows the relationship between the clock quality (σ_{emprcl} and σ_{STD}) and the improvement factor f of the kinematic height estimates with a relative clock constraint of 2 mm. The IGS/CODE/ESA clock records of the H-Masers listed in Table 1 in February 2011 were used for the plots. We see that the number of improvement factors below 1 increases with an increasing σ_{emprcl} and σ_{STD} . For the clocks with $\sigma_{emprcl} < 15\text{ ps}$ and $\sigma_{STD} < 50\text{ ps}$, the improvement factors are in 98 % of the time above 1, thereof 49 % above 1.5.

In order to analyze the variations in kinematic heights over various time intervals, the MDEV of the kinematic height estimates for station ONSA on February 1st, 2011 using different stochastic clock models were computed (see Fig. 10). The black line indicates the MDEV of the kinematic height

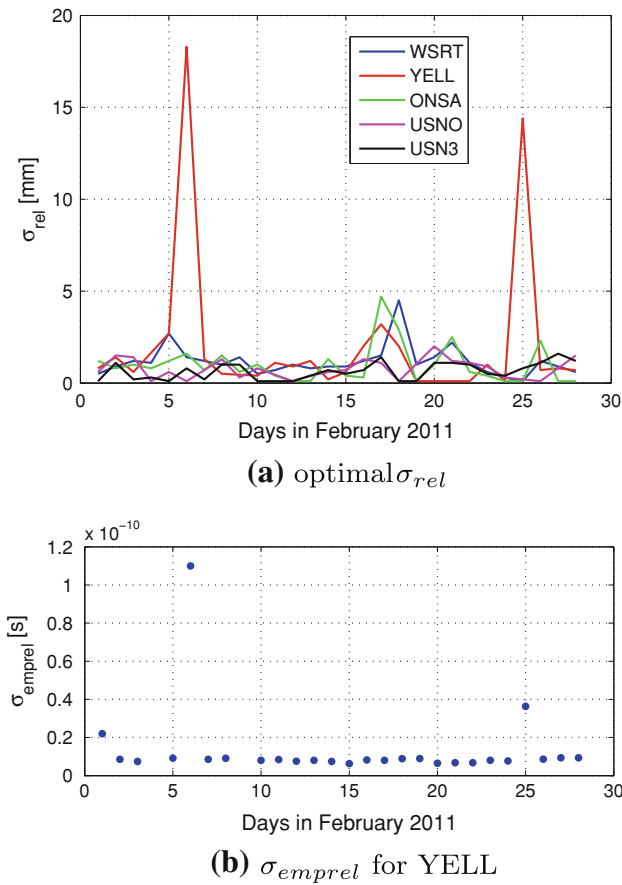


Fig. 8 The optimal relative sigma σ_{rel} for **a** five very stable H-masers in February 2011 and **b** the empirical relative sigma σ_{emprel} for the H-maser at station YELL during February 2011

estimates obtained without any relative clock constraints. The magenta and the blue line corresponding to epoch-to-epoch relative constraints of 1.2 mm (4 ps) and the

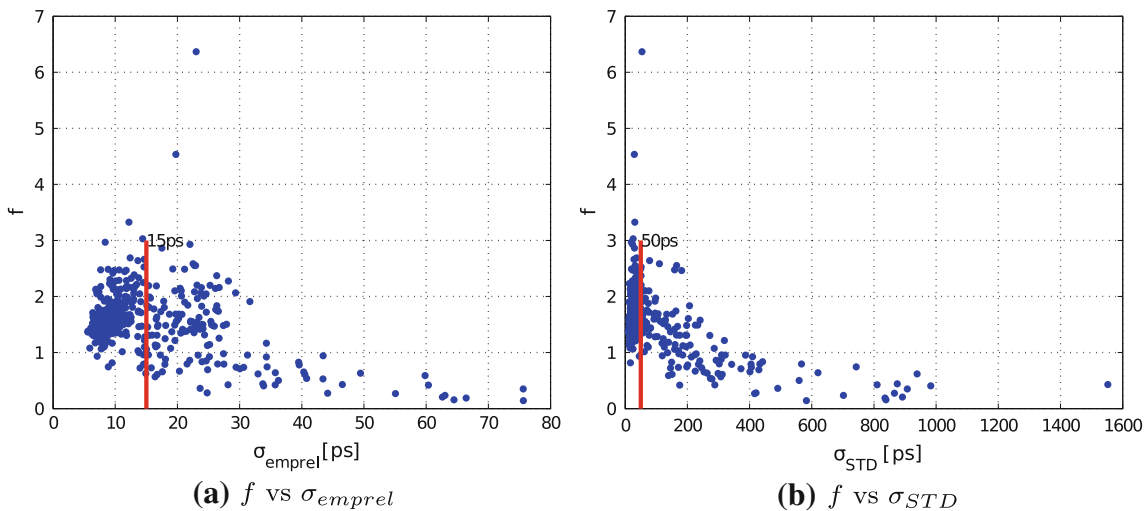


Fig. 9 Relationship between the improvement factors f with a relative clock constraint of 2 mm and **a** the empirical relative sigma σ_{emprel} and **b** the standard deviation from a linear polynomial σ_{STD} using the IGS/CODE/ESA clock records of 16 H-Masers in February 2011.

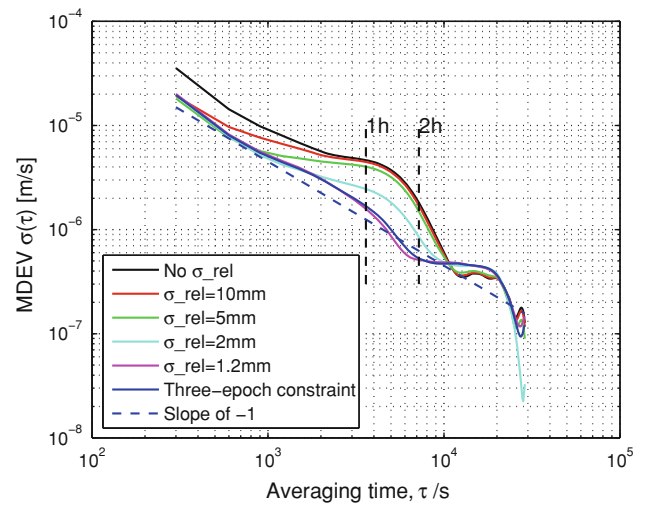


Fig. 10 MDEV of kinematic height estimates for station ONSA using different relative constraints on February 1st, 2011

three-epoch constraints, respectively, show huge improvements in precision of the kinematic height estimates ranging from 5 min to about 3 h. It can also be seen that the quality of the kinematic height estimates is somewhat degraded for time intervals between approximately 30 min and 3 h compared to the slope of -1 for typical flicker noise (blue dashed line). Since the ZPDs were estimated with a time resolution of 2 h, this limited time resolution might be the cause of this degradation.

To verify this, different sampling intervals for the ZPD parameters were tested. The resulting MDEV of kinematic height estimates for ONSA are shown in Fig. 11 applying (a) no clock constraints or (b) relative constraints of 2 mm (6.7 ps) between subsequent clock parameters. Compared to the slope of -1 for typical flicker noise in the MDEV

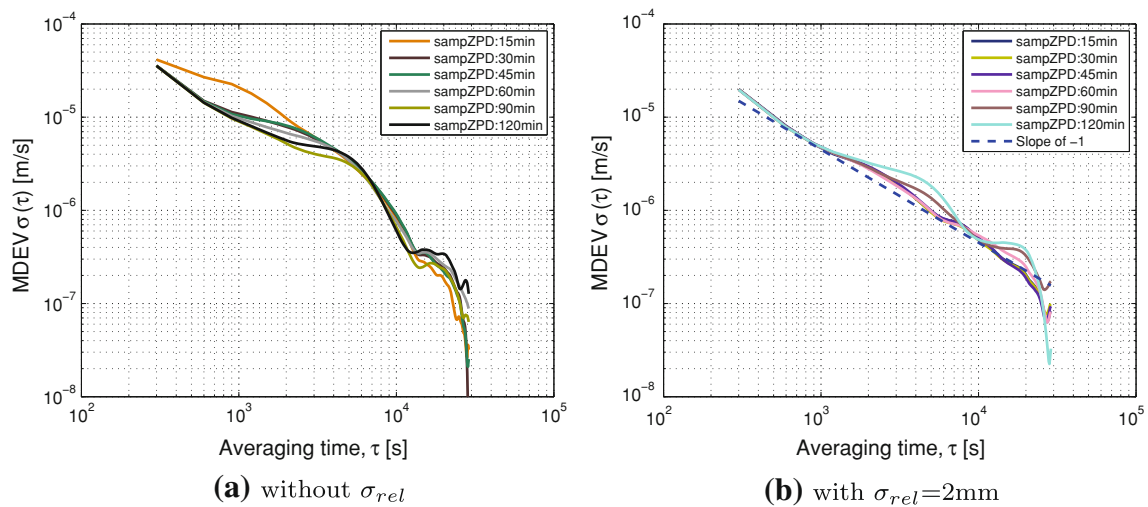


Fig. 11 MDEV of kinematic height estimates for ONSA using **a** no relative constraints and **b** relative constraints of 2 mm between subsequent clock epochs on February 1st, 2011. The troposphere ZPD parameters were set up with different sampling intervals

(see blue dashed line in Fig. 11b), obvious deviations can be observed for long time intervals. By decreasing the sampling intervals of the ZPD parameters, these deviations are considerably reduced, showing that the modeling deficiencies due to the insufficient time resolution of the troposphere parameters deteriorate the kinematic height estimates for large averaging times. The cases with a ZPD time resolution higher than 60 min are overwritten by the 60 min case. This means that no degradation of the kinematic heights takes place even if a 15 min time resolution for the ZPDs is used. The relative clock constraints thus allow for a higher temporal resolution of the troposphere parameters, which may be advantageous in the case of fast changing weather conditions. In contrast, in the case without applying relative clock constraints (see Fig. 11a), the increase in the number of ZPDs eventually (15 min ZPD resolution) leads to a degradation of the kinematic height estimates at averaging intervals below about 1 h. An offset can generally be observed between Fig. 11a, b. It shows the positive effect of an appropriate relative clock constraint on the kinematic height estimates.

Experiments have also been performed with respect to even stronger relative constraints, e.g., 1.2 mm (4 ps), which corresponds to the optimal σ_{rel} for the H-maser at ONSA (see Fig. 10). However, the benefits from changing the sampling interval of ZPD parameters are not obvious any more. The improvements are very similar to the case using a constraint of 2 mm (6.7 ps) and a 60 min ZPD interval.

5 Estimation of kinematic station coordinates with simulated data

In order to verify the results obtained with real data, GPS code and phase observations on both frequencies were simulated

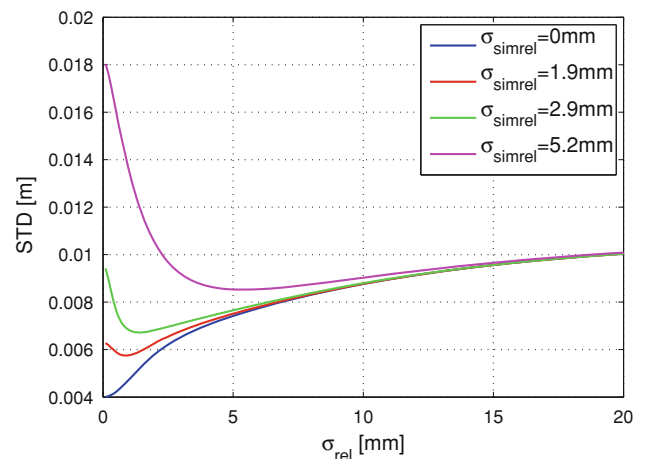


Fig. 12 Standard deviation of the kinematic height estimates derived from simulated GPS data with realistic receiver clock behavior using different relative constraints on subsequent clock parameters. The CODE clock RINEX files were used for simulation of the receiver clocks

with a pre-defined receiver clock behavior, a phase observation noise of 2 mm and a code observation noise of 20 cm using a modified version of Bernese GPS Software 5.0 (Dach et al. 2007). The simulated receiver clocks were generated with an offset, a drift and the deviations of the H-masers at WSRT (Westerbork Synthesis Radio Telescope, Westerbork, Netherlands), ONSA and HOB2 (Hobart AU016, Hobart, Australia) from a linear clock behavior amounting to an RMS of 14.7, 35.3 and 44.3 ps, respectively, on February 1st, 2011. After multiplication with the speed of light, the RMS of the epoch-to-epoch difference σ_{emprcl} of these three real clocks amount to 1.9 mm (6.3 ps), 2.9 mm (9.7 ps) and 5.2 mm (17.3 ps), respectively.

In Fig. 12 we see the results of the simulations using different relative constraints for the receiver clocks. Different

colors represent different clock qualities. We see that in this simulated case the stability of the height estimates as a function of the relative clock constraints behaves very similar to the real data case (see Fig. 7). We also see that the better the clock quality, the smaller the optimal σ_{rel} . The optimal σ_{rel} is below 2 mm (6.7 ps) for stable clocks (with $\sigma_{\text{simrel}} = 1.9$ mm (6.3 ps) and $\sigma_{\text{simrel}} = 2.9$ mm (9.7 ps)) and above 2 mm (6.7 ps) for the clock with $\sigma_{\text{simrel}} = 5.2$ mm (17.3 ps). The blue line represents the clock with a perfect behavior, i.e., without any stochastic component. For the perfect clock, the stronger the relative constraints are, the better performance we can get for the kinematic height estimates, even for very strong constraints.

6 Summary and conclusions

The kinematic coordinates derived from an PPP solution using phase measurements typically show an accuracy at cm-level in horizontal and at sub-decimeter level in vertical direction (Geng et al. 2010). This means that it is more difficult to detect real motions of a receiver in height than in horizontal positions. This situation can considerably be changed, if high-stability H-masers are connected to the receiver. Using a simple deterministic model (e.g., a linear polynomial) and relative constraints with an appropriate weight between subsequent epochs (e.g., 2 mm or 6.7 ps) for such a clock, the kinematic solutions can be significantly improved in the less accurate vertical direction, namely, by up to a factor of 2 to 3. The optimal weight for the relative constraints between subsequent clock epochs, which leads to the best kinematic solution, depends heavily on the quality of the clock considered. For very stable H-masers, i.e., for H-masers with a standard deviation lower than 50 ps after removing a linear polynomial and an RMS σ_{emprel} of the epoch-to-epoch clock differences smaller than 15 ps, the optimal relative constraint typically lies between 0 and 2 mm (0 and 6.7 ps). Taking the 16 investigated H-Masers (see Table. 1) in February 2011 for example, for all the clocks that have passed the criteria that are mentioned above ($\sigma_{\text{emprel}} < 15$ ps and $\sigma_{\text{STD}} < 50$ ps), 98 % of the improvement factors are above 1, 49 % thereof above 1.5. It should be noticed that the σ_{emprel} derived from the GPS estimates is noisier than the real clock. It can only be considered as a measure for the clock quality, but is not directly related to the optimal relative sigma.

Relative constraints between subsequent *and* near-subsequent epochs using weights derived from the MDEV of clock records available from IGS, CODE or ESA is also a good and safe choice for stabilizing the kinematic solutions in the vertical direction. In this way, the stability of the kinematic height estimates can also be improved by up to a factor of approximately 2 to 3. Taking the 16 investigated H-Masers (see Table. 1) in February 2011 for example, for all the clocks that have passed the criteria that are mentioned

above ($\sigma_{\text{emprel}} < 15$ ps and $\sigma_{\text{STD}} < 50$ ps), 99 % of the improvement factors are above 1, 44 % thereof above 1.5.

It is clear that the improvement in the repeatability of the kinematic heights (i.e. in changes of the kinematic heights) is roughly limited to time intervals, during which the receiver clock does not deviate by more than about 50 ps from a linear behavior.

Most benefit from the methods presented here are therefore to be expected in the quantification and detection of small height changes at cm-level over short time intervals (a few hours to one day). Prominent and important examples are certainly earthquake ground motions and displacements, tsunami GPS buoys and land slides, provided that H-Masers or other clocks of similar performance are getting cheaper and less sensible to the environment in the future.

Because of the high correlation of the troposphere zenith delays with the station height estimates, the sampling intervals used for the ZPD estimation is always a critical issue in kinematic positioning. Experiments have shown that with an appropriate relative clock constraint increasing the sampling resolution of the ZPD parameters from 2 h to one or even half an hour clearly improves the stability of kinematic height estimates. Therefore, we may expect that clock constraints allow it to estimate troposphere parameters with a much higher temporal resolution without suffering from the high correlation between troposphere and heights, an important aspect for the determination of water vapor on ships or buoys to cover ocean areas.

It should be mentioned that no significant improvements can be obtained in the PPP solutions applying different clock models, if only one set of coordinates is estimated per day (Orliac et al. 2012). Tests have also shown that the modeling of the receiver clocks on the ground does not have a significant impact on GPS orbits and Earth rotation parameters (ERPs).

In the future, with the progress made in the field of high-performance frequency standards, more and more stable and cheap clocks will become available and the use of clock modeling will become more and more important. With the completion of the Galileo constellation in the near future, it will be possible to also make use of very stable satellite clocks. The stability of such clocks was studied by, e.g., Montenbruck et al. (2012), for the case of the GIOVE-B satellite carrying a H-Maser. Since receiver clock modeling, as mentioned above, does not have much effect on global parameters, one can conclude that making use of the very good receiver clocks improves the receiver-specific parameters (like heights and ZPDs), whereas global or satellite-specific parameters (like earth rotation parameters and satellite orbits) show no or only very small improvements. It is to be expected in analogy, therefore, that the constraining of the high-performance satellite clocks will mainly lead to improvement in satellite-specific parameters (e.g. orbital parameters, decorrelation of

orbital parameters and satellite clock corrections). Improved separation of the highly correlated satellite orbits and satellite clock parameters may help in future to better assess the deficiencies in the orbit modeling, especially in the solar radiation pressure models.

In the far future, as the clocks developed for receivers and satellites are getting more and more stable as described in this paper, the stochastic modeling of clocks over longer and longer time spans will become an integral task of high-precision GNSS analyses, leading to improvements in both, receiver- and satellite-specific parameters.

Acknowledgments This work was funded by ESA as part of the project (Satellite and Station Clock Modeling for GNSS, Reference: AO/1-6231/09/D/SR). We would like to thank the partner institutions: Astronomical Institute, University of Bern (AIUB) and Institute for Astronomical and Physical Geodesy (IAPG), Technische Universität München (TUM), especially Etienne Orliac (AIUB) for providing the pre-processed observation data.

References

- Allan DW, Barnes JA (1981) A modified "Allan variance" with increased oscillator characterization ability. In: Proceedings of the 35th Annual Frequency Control Symposium, Philadelphia, USA, 27–29 May, pp 470–475
- Allan DW (1987) Time and frequency (time-domain) characterization, estimation and prediction of precision clocks and oscillators. *IEEE Trans Ultrason Ferroelectrics Freq Control* 34(6):647–654. doi:10.1109/T-UFFC.1987.26997
- Bock H, Dach R, Jäggi A, Beutler G (2009) High-rate GPS clock corrections from CODE: support of 1 Hz applications. *J Geod* 83(11):1083–1094. doi:10.1007/s00190-009-0326-1
- Boehm J, Werl B, Schuh H (2006) Troposphere mapping functions for GPS and very long baseline interferometry from European Centre for Medium-Range Weather Forecasts operational analysis data. *J Geophys Res* 111(B2):B02406. doi:10.1029/2005JB003629
- CLKLOG (2012) A summary file of the deployment history for GPS receiver, antenna, frequency standards, and other equipment at IGS stations. <ftp://igs.jpl.nasa.gov/igs/station/general/loghist.txt>
- Dach R, Beutler G, Hugentobler U, Schaer S, Schildknecht T, Springer T, Dudle G, Prost L (2003) Time transfer using GPS carrier phase: error propagation and results. *J Geod* 77(1–2):1–14. doi:10.1007/s00190-002-0296-z
- Dach R, Hugentobler U, Fridez P, Meindl M (2007) Bernese GPS Software Version 5.0. Astronomical Institute, University of Bern, Bern
- Dach R, Brockmann E, Schaer S, Beutler G, Meindl M, Prange L, Bock H, Jäggi A, Ostini L (2009) GNSS processing at CODE: status report. *J Geod* 83(3–4):353–365. doi:10.1007/s00190-008-0281-2
- Dow J, Neilan R, Rizos C (2009) The international GNSS Service in a changing landscape of Global Navigation Satellite Systems. *J Geod* 83(3–4):191–198. doi:10.1007/s00190-008-0300-3
- Dupuis RT, Lynch TJ, Vaccaro JR, Watts ET (2010) Rubidium Frequency Standard for the GPS IIF Program and Modifications for the RAFSMOD Program. In: Proc ION GNSS, 2010, 781–788, Oregon, Portland
- Ge M, Gendt G, Dick G, Zhang FP, Rothacher M (2006) A new data processing strategy for huge GNSS global networks. *J Geod* 80(4):199–203. doi:10.1007/s00190-006-0044-x
- Geng J, Teferle F, Meng X, Dodson A (2010) Kinematic precise point positioning at remote marine platforms. *GPS Solut* 14(4):343–350. doi:10.1007/s10291-009-0157-9
- Hugentobler U (2004) CODE high rate clocks. IGS Mail No.4913, IGS Central Bureau Information System
- Jäggi A, Prange L, Hugentobler U (2011) Impact of covariance information of kinematic positions on orbit reconstruction and gravity field recovery. *Adv Space Res* 47(9):1472–1479. doi:10.1016/j.asr.2010.12.009
- Lichten SM, Border JS (1987) Strategies for high-precision global positioning system orbit determination. *J Geophys Res* 92(B12):12751–12762. doi:10.1029/JB092iB12p12751
- Montenbruck O, Steigenberger P, Schönemann E, Hauschild A, Hugentobler U, Dach R, Becker M (2012) Flight Characterization of New Generation GNSS Satellite Clocks. *Nav J Ins Nav* 59(4):291–302. doi:10.1002/navi.22
- Orliac E, Dach R, Wang K, Rothacher M, Voithenleitner D, Hugentobler U, Heinze M, Svehla D (2012) Deterministic and stochastic receiver clock modeling in precise point positioning. EGU General Assembly 2012, 22–27 April, 2012, Austria, Vienna, p 7199
- Ray J, Gurtner W (2010) RINEX extensions to handle clock information. http://igs.jpl.nasa.gov/igs/data/format/rinex_clock302.txt
- Ray J, Senior K (2003) IGS/BIPM pilot project: GPS carrier phase for time/frequency transfer and timescale formation. *Metrologia* 40(3):270–288. doi:10.1088/0026-1394/40/3/307
- Rothacher M, Beutler G (1998) The role of GPS in the study of global change. *Phys Chem Earth* 23(9–10):1029–1040. doi:10.1016/S0079-1946(98)00143-8
- Senior K, Koppang P, Ray J (2003) Developing an IGS time scale. *IEEE Trans Ultrason Ferroelect Freq Control* 50(6):585–593. doi:10.1109/TUFFC.2003.1209545
- Wang K, Rothacher M (2011) GNSS clock modelling and estimation. Swiss National Report on the Geodetic Activities in the years 2007 to 2011, pp 30–33
- Weinbach U, Schön S (2009) Evaluation of the clock stability of geodetic GPS receivers connected to an external oscillator. In: Proc ION GNSS 2009, pp 3317–3328, Savannah, GA, USA
- Weinbach U, Schön S (2011) GNSS receiver clock modeling when using high-precision oscillators and its impact on PPP. *Adv Space Res* 47(2):229–238. doi:10.1016/j.asr.2010.06.031
- Zumberge JF, Hefflin MB, Jefferson DC, Watkins MM, Webb FH (1997) Precise point positioning for the efficient and robust analysis of GPS data from large networks. *J Geophys Res* 102(B3):5005–5017. doi:10.1029/96JB03860